

Hydrothermal synthesis and structures of three new copper complexes: $[\{\text{Cu}(2,2'\text{-bipy})_2\}_2(\beta\text{-Mo}_8\text{O}_{26})]$, $[\{\text{Cu}(\text{py})_3\}_2\{\text{Cu}(\text{py})_2\}_2(\alpha\text{-Mo}_8\text{O}_{26})]$ and $[\text{Cu}(\text{py})_2]_4[(\text{SO}_4)\text{Mo}_{12}\text{O}_{36}]^\dagger$

Wenbin Yang, Canzhong Lu* and Honghui Zhuang

The State Key Laboratory of Structural Chemistry,
Fujian Institute of Research on the Structure of Matter, The Chinese Academy of Sciences,
Fuzhou, Fujian, 350002, P.R. China. E-mail: czlu@ms.fjirsm.ac.cn

Received 17th December 2001, Accepted 22nd May 2002

First published as an Advance Article on the web 20th June 2002

Two interesting organic–inorganic hybrid solids $[\{\text{Cu}(2,2'\text{-bipy})_2\}_2(\beta\text{-Mo}_8\text{O}_{26})]$ (**1**), $[\{\text{Cu}(\text{py})_3\}_2\{\text{Cu}(\text{py})_2\}_2(\alpha\text{-Mo}_8\text{O}_{26})]$ (**2**), and a new two-electron-reduced Keggin-core compound $[\text{Cu}(\text{py})_2]_4[\text{Mo}_{12}\text{O}_{36}(\text{SO}_4)]$ (**3**), were synthesized by hydrothermal methods and structurally characterized by X-ray diffraction. The structure of **1** consists of discrete $[\{\text{Cu}(2,2'\text{-bipy})_2\}_2(\beta\text{-Mo}_8\text{O}_{26})]$ clusters, constructed from $\beta\text{-}[\text{Mo}_8\text{O}_{26}]^{4-}$ subunits covalently bonded to two $[\text{Cu}(2,2'\text{-bipy})_2]^{2+}$ coordination cations *via* bridging oxo groups that connect two adjacent molybdenum sites. The structure of **2** consists of heterometallic dodecanuclear clusters, $[\{\text{Cu}(\text{py})_3\}_2\{\text{Cu}(\text{py})_2\}_2(\alpha\text{-Mo}_8\text{O}_{26})]$, connected *via* $\pi\text{-}\pi$ stacking contacts into an extended 1-D chain. Each $[\alpha\text{-Mo}_8\text{O}_{26}]^{4-}$ anion forms weak covalent interactions to two $[\text{Cu}(\text{py})_3]^+$ and two $[\text{Cu}(\text{py})_2]^+$ units through terminal oxo groups of the octamolybdate cluster. A new compound $[\text{Cu}(\text{py})_2]_4[\text{Mo}_V\text{Mo}_{10}\text{O}_{36}(\text{SO}_4)]$ (**3**), with two-electron-reduced Keggin anions, was unexpectedly obtained from the similar hydrothermal treatment of **2**. Compounds **1–3** are of interest due to their unusual Cu-coordination geometries; trigonal bipyramidal Cu(II), distorted tetrahedral, T-shaped trigonal, and linear Cu(I) are observed, and in **2**, two distinct Cu(I)-coordination geometries are observed in the same structure!

Introduction

Stimulated by the wide range of topologies and driven by potential applications in catalysis, biology, medicine and materials science, transition metal oxides (so-called polyoxometalates) have attracted particular interest for a long time.¹ However, the driving force for the formation of these polyoxometalate species is not well understood, and commonly described as self-assembly. This makes it rather difficult to straightforwardly prepare such compounds, even in some very simple cases. Based on the fact that polyoxometalate frameworks with high electronic density can act as unusually effective ligands to coordinate second transition metals, as reviewed by Zubieta *et al.*,² important progress has been made recently on the coordination chemistry of polyoxoanions with classical transition metal coordination complexes or fragments. Previous studies have demonstrated that the transition metal coordination complexes may adopt a variety of roles: (1) as charge-compensating coordinated units, *e.g.* $[\text{Zn}(2,2'\text{-bipy})_3]_2[\text{V}_4\text{O}_{12}]$;³ (2) as covalently bound subunits of the metal oxide framework itself, *e.g.* $[\{\text{Ni}(o\text{-phen})_2\}(\xi\text{-Mo}_8\text{O}_{26})]$;⁴ (3) as inorganic bridging “ligands” linking polyanion clusters into infinite extended networks, as shown for $[\text{Cu}(\text{en})_2]_3[\text{V}_{15}\text{O}_{36}\text{Cl}]$ ⁵ and $[\{\text{Cu}(4,7\text{-phen})_3\}_2(\text{Mo}_{14}\text{O}_{45})]$.⁶

Of the various polyoxometalate structures, the most interesting one is the octamolybdate family with a variety of structural isomers including α -, β -, and γ -octamolybdates,⁷ the δ -isomer in $[(\eta\text{-C}_5\text{Me}_5\text{Rh})_2(\mu\text{-SCH}_3)_3]_4[(\text{Mo}_8\text{O}_{26})\cdot 2\text{CHCN}]$ ⁸ and $[\{\text{Cu}(4,4'\text{-bipy})_4(\text{Mo}_8\text{O}_{26})\}]$,⁹ the ϵ -isomer in $[\{\text{Ni}(\text{H}_2\text{O})_2(4,4'\text{-bipy})_2\}_2(\text{Mo}_8\text{O}_{26})]$,⁹ and ζ -isomers in $[\{\text{M}(\text{phen})_2\}(\xi\text{-Mo}_8\text{O}_{26})]$ ($\text{M} = \text{Ni}$ or Co).⁴ These octamolybdate isomers are versatile inorganic building blocks for constructing new organic–inorganic hybrid

materials with desirable properties.² A large number of octamolybdate-based copper complexes have been synthesized and characterized, in which copper centers adopt square pyramidal coordination environments for Cu(II) or tetrahedral geometries for Cu(I). Here, we report the hydrothermal synthesis and characterization of three new molecular clusters, where the copper coordination cations form a covalent attachment to the oxide skeletal backbone (for **1** and **2**), or act as a charge-compensating coordinated unit (for **3**). Compounds **1–3** are of interest due to the unusual Cu-coordination geometries; trigonal bipyramidal Cu(II), distorted tetrahedral, T-shaped trigonal, and linear Cu(I); in **2**, two distinct Cu(I)-coordination geometries are observed in the same structure! In addition, in the structure of **1**, a $\beta\text{-Mo}_8\text{O}_2$ cluster bonds covalently to two copper(II) coordination complexes *via* bridging oxo groups; such an unusual linking fashion is, to the best of our knowledge, unique in the coordination chemistry of octamolybdates with transition metal complexes and even in the whole coordination chemistry of molybdenum-oxo clusters.

Experimental

Reagents were purchased from Aldrich Chemical Co. and used without further purification. All of the syntheses were carried out in polytetrafluoroethylene-lined stainless steel containers under autogenous pressure. Elemental analyses of C and H were performed with an EA1110 CHNS-0 CE elemental analyzer. All IR (KBr pellet) spectra were recorded on a Nicolet Magna 750FT-IR spectrometer, while ESR spectra were measured with a Bruker ESR-420 spectrometer (X-band).

Synthesis

$[\{\text{Cu}(2,2'\text{-bipy})_2\}_2(\beta\text{-Mo}_8\text{O}_{26})]$ (1**)**. A mixture of $\text{MoO}_3\cdot\text{H}_2\text{O}$ (0.32 g), $(\text{NH}_4)_6\text{Mo}_7\text{O}_{24}\cdot 4\text{H}_2\text{O}$ (0.41 g), $\text{CuSO}_4\cdot 5\text{H}_2\text{O}$ (0.25 g), 2,2'-bipy (0.40 g) and H_2O (10 ml) was sealed in a Teflon-lined

[†] Electronic supplementary information (ESI) available: ESR spectra of **1** and **3**, IR spectra of **1–3**. See <http://www.rsc.org/suppdata/dt/b1/b111480h/>

Table 1 Crystallographic data for $[\{\text{Cu}(2,2'\text{-bipy})_2\}_2(\beta\text{-Mo}_8\text{O}_{26})]$ (**1**), $[\{\text{Cu}(\text{py})_3\}_2\{\text{Cu}(\text{py})_2\}_2(\alpha\text{-Mo}_8\text{O}_{26})]$ (**2**), and $[\text{Cu}(\text{py})_2]_4[\text{Mo}_{12}\text{O}_{36}(\text{SO}_4)]$ (**3**)

	1	2	3
Formula	$\text{C}_{40}\text{H}_{32}\text{Cu}_2\text{Mo}_8\text{N}_8\text{O}_{26}$	$\text{C}_{50}\text{H}_{50}\text{Cu}_4\text{Mo}_8\text{N}_{10}\text{O}_{26}$	$\text{C}_{40}\text{H}_{40}\text{Cu}_4\text{Mo}_{12}\text{N}_8\text{O}_{40}\text{S}$
FW	1935.34	2228.68	2710.30
Crystal size/mm	$0.50 \times 0.46 \times 0.45$	$0.66 \times 0.36 \times 0.18$	$0.38 \times 0.30 \times 0.30$
Crystal color	Sapphire	Red	Black
Crystal system	Orthogonal	Triclinic	Triclinic
Space group	$Pna2(1)$	$P\bar{1}$	$P\bar{1}$
$a/\text{\AA}$	24.2245(5)	11.0467(2)	12.1346(2)
$b/\text{\AA}$	18.33150(10)	13.6580(2)	13.3362(3)
$c/\text{\AA}$	11.9118(2)	13.7406(2)	13.3760(3)
$\alpha/^\circ$	90	67.0290(10)	107.8540(10)
$\beta/^\circ$	90	67.3310(10)	115.5690(10)
$\gamma/^\circ$	90	68.54	103.0490(10)
$V/\text{\AA}^3$	5289.69(14)	1703.72	1689.23(6)
Z	4	1	1
T/K	293(2)	293(2)	293(2)
$\mu(\text{Mo-K}\alpha)/\text{mm}^{-1}$	2.710	2.722	3.504
$F(000)$	3720	1080	1292
R^a	0.0392	0.0346	0.0442
R_w^b	0.0801	0.0924	0.1149

$$^a R = \Sigma(|F_o| - |F_c|)/\Sigma|F_o|, \quad ^b R_w = [\Sigma w(F_o^2 - F_c^2)^2/\Sigma w(F_o^2)]^{0.5}$$

stainless steel reactor and heated at 170 °C for two days. After the reaction system was slowly cooled down to room temperature, sapphire block crystals of **1** were obtained in high yield (86% based on Mo). Anal. calc.: C, 24.82; H, 1.67; N, 5.79; Cu, 6.57; Mo, 39.66%. Found: C, 24.76; H, 1.63; N, 5.82; Cu, 6.54; Mo, 39.78%. Characteristic IR bands for **1** (KBr pellet, ν/cm^{-1}): 3082(s) $\nu(\text{C-H})$, 1601(s), 1574(w), 1497(m), 1473(m), 1446(vs), 1315(m), 1176(m), 1032(m), 945(vs), 926(s), 910(vs), 849(vs), 779(m), 762(s), 721(vs), 692(vs), 550(s), 409(m).

[\{Cu(py)₃\}_2\{Cu(py)₂\}_2(\alpha-Mo₈O₂₆)] (2**).** A mixture of Na₂MoO₄·2H₂O (0.48 g), CuSO₄·5H₂O (0.25 g), nicotinic acid (py-3-CO₂H, 0.36 g) and H₂O (15 ml) was sealed in a Teflon-lined stainless steel reactor and heated at 195 °C for 4 days, then slowly cooled to room temperature to give red crystals of **2** in high yield (90% based on Mo). Anal. calc.: C, 26.95; H, 2.26; N, 6.28; Cu, 11.41; Mo, 34.44%. Found: C, 26.86; H, 2.23; N, 6.35; Cu, 11.39; Mo, 34.41%. Characteristic IR bands for **2** (KBr pellet, ν/cm^{-1}): 3060(s) $\nu(\text{C-H})$, 1605(s), 1597(s), 1483(m), 1570(w), 1443(vs), 1213(w), 1153(w), 1066(m), 1039(w), 955(s), 922(vs), 906(vs), 839(s), 812(vs), 754(m), 696(vs), 661(vs), 561(m).

[Cu(py)₂]₄[Mo₁₂O₃₆(SO₄)] (3**).** Similar hydrothermal treatment of Na₂MoO₄·2H₂O (0.36 g), CuSO₄·5H₂O (0.15 g), nicotinic acid (0.24 g) and H₂O (8.1 ml) for 4 days at 195 °C gave deep black crystals of **3** in relatively low yield (30% based on Mo). Anal. calc.: C, 17.73; H, 1.49; N, 4.13; Cu, 9.38; Mo, 42.78; S, 1.18%. Found: C, 17.68; H, 1.52; N, 4.21; Cu, 9.33; Mo, 42.65; S, 1.21%. Characteristic IR bands for **3** (KBr pellet, ν/cm^{-1}): 3099(m), 3077(m) $\nu(\text{C-H})$, 1606(s), 1568(w), 1485(w), 1446(s), 1217(w), 1155(w), 1059(s), 957(vs), 928(s), 800(vs), 758(s), 694(s), 648(m), 503(w).

X-Ray crystallography

Structural measurements for compounds **1–3** were performed on a Siemens SMART CCD diffractometer with graphite monochromated Mo-K α radiation ($\lambda = 0.71073 \text{ \AA}$) at room temperature. In all cases, an empirical absorption correction by SADABS²³ was applied to the intensity data. The structures were solved by direct methods, successive Fourier difference syntheses, and refined by full matrix least-squares minimization of $(\Sigma w(F_o - F_c)^2)$ with anisotropic thermal parameters for all non-hydrogen atoms. All hydrogen atoms were allowed for riding atoms. Crystal parameters and other experimental details of the data collection for **1–3** are summarized in Table 1.

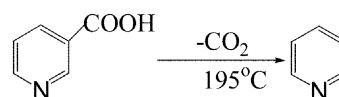
CCDC reference numbers 175398–175400.

See <http://www.rsc.org/suppdata/dt/b1/b111480h/> for crystallographic data in CIF or other electronic format.

Results and discussion

Although due to the fact that low-temperature hydrothermal synthesis (140–220 °C) depends on “self-assembly” and therefore frequently gives polyphase products or suffers from problems such as poor yields or reproducibility problems, compounds **1** and **2** were obtained in high yield (86 and 90%, respectively). The sapphire coloration of the crystals of **1** indicates that it is a Cu(II) complex, which is supported by valence sum calculations¹⁰ and an ESR spectrum exhibiting an isotropic signal with $g = 2.0766$, and $A = 255 \text{ G}$ at room temperature. The crystals of **3** are black, indicating that the Mo atoms are in mixed valence, which is also supported by valence sum calculations and the room temperature ESR spectrum. The ESR spectrum for **3** exhibits a paramagnetic signal with $g = 1.9982$ and $A = 30.33 \text{ G}$; six hyperfine lines caused by the coupling of the unpaired electrons with the nuclear spin ($I = 5/2$) are observed. Valence sum calculations confirm that the average oxidation state of the Mo sites in **3** is +5.4, rather than +6 for the fully oxidized forms in **1** and **2**. Similarly, valence sum calculations on the Cu sites in **2** and **3** provide an average oxidation of +1.0, suggesting that complex **2** may be described as an $[\alpha\text{-Mo}_8\text{O}_{26}]^{4-}$ polyoxoanion coordinated to two $[\text{Cu}(\text{py})_3]^+$ and two $[\text{Cu}(\text{py})_2]^+$ subunits, **3** as a $[(\text{SO}_4)\text{Mo}^{\text{V}}_2\text{Mo}^{\text{VI}}_{10}\text{O}_{36}]^{4-}$ anion charge neutralized by four $[\text{Cu}(\text{py})_2]^+$ cations.

The formation of **2** and **3** have three key aspects: (1) COO[−] group loss from nicotinic acid, (2) reduction of Cu²⁺ and (3) self-assembly crystallization. Since no pyridine (py) was used to synthesize **2** and **3**, the py ligands must result from the following decomposition reaction of nicotinic acid which occurs under 195 °C:



The resultant pyridine acts as an effective agent to reduce Cu(II) to Cu(I), and then the reduced Cu(I) is coordinated by additional pyridine to form complex cations $[\text{Cu}(\text{py})_3]^+$ and $[\text{Cu}(\text{py})_2]^+$, which self-assemble with $[\alpha\text{-Mo}_8\text{O}_{26}]^{4-}$ in crystal forms and precipitate out from the hydrothermal solution. It is a common phenomenon that high oxide-state metals are

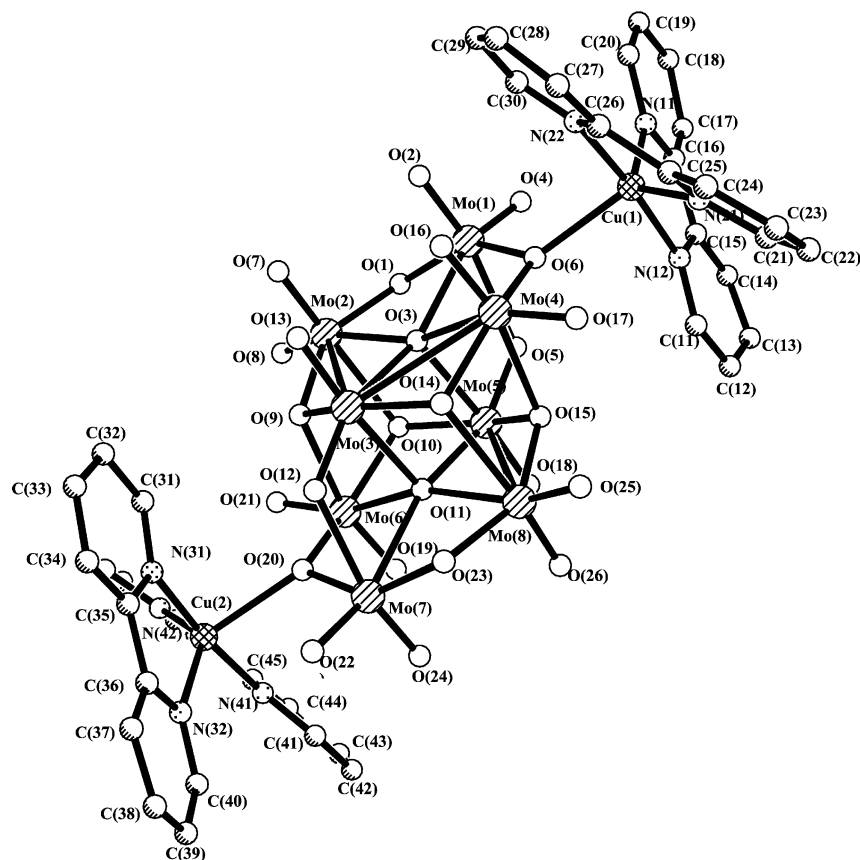


Fig. 1 Molecular structure of **1**.

reduced by organic amines under hydrothermal conditions. In **3**, $[\text{Cu}(\text{py})_2]^+$ coordination complexes are only introduced as counterions.

Can pyridine be used to prepare **2** and **3** instead of nicotinic acid? Various parallel reactions have been performed under hydrothermal conditions using pyridine in place of nicotinic acid. However, the results of the elemental analyses and X-ray crystallography reveal that only **3** can be obtained in the presence of excess pyridine. In addition, various procedures have been carried out to study the effects of changing the temperature and the molar ratios of the starting materials. No crystals for **2** or **3** could be obtained when the corresponding reagents were heated at 180 °C for 4 days. This shows that both the reduction of Cu(II) to Cu(I) and their further aggregation to **2** or **3** occurs at high temperature. It is also noteworthy that the stoichiometry is important in determining the products and yields: red crystals of **2** were mainly precipitated when $\text{CuSO}_4 : \text{py}-3\text{-CO}_2\text{H} \geq 1 : 3$; the two-electron-reduced Keggin derivative **3** was isolated as deep black prisms with a small amount of green amorphous solid when $\text{CuSO}_4 : \text{py}-3\text{-CO}_2\text{H} \leq 1 : 3.2$ and $(\text{Na}_2\text{MoO}_4 + \text{CuSO}_4) : \text{py}-3\text{-CO}_2\text{H} \leq 1 : 1$.

Compounds **1–3** are insoluble in water and most organic solvents. IR spectra of **1–3** exhibit characteristic bands for Mo=O and organic donors of 2,2'-bipy or pyridine. The structure of **1** consists of discrete heterometallic decanuclear clusters $[\{\text{Cu}(2,2'\text{-bipy})_2\}(\beta\text{-Mo}_8\text{O}_{26})]$ (Fig. 1, Table 2). The octamolybdate anion in **1** is the $\beta\text{-}[\text{Mo}_8\text{O}_{26}]^{4-}$ isomer, consisting of eight edge-shared MoO_6 octahedra and four kinds of Mo–O bonds: Mo–O(t), 1.681(9)–1.709(9) Å, Mo–O(μ), 1.732(8)–2.262(9) Å, Mo–O(μ_3), 1.934(8)–2.411(8) Å, Mo–O(μ_5), 2.165(8)–2.488(8) Å.

Each $\beta\text{-}[\text{Mo}_8\text{O}_{26}]^{4-}$ unit forms covalent interactions with two $[\text{Cu}(2,2'\text{-bipy})_2]^{2+}$ units through bridging oxo groups of the octamolybdate unit with Cu–O distances of 2.239(9) and 2.264(9) Å. Each five-coordinated Cu(II) ion is of a slightly distorted trigonal bipyramid, $\text{N}(\text{CuON}_2)\text{N}$, of which two apical

Table 2 Selected bond lengths (Å) and angles (°) for $[\{\text{Cu}(2,2'\text{-bipy})_2\}_2(\beta\text{-Mo}_8\text{O}_{26})]$ (**1**)

Cu(1)–N(11)	1.978(11)	Cu(2)–N(31)	1.960(11)
Cu(1)–N(22)	1.979(10)	Cu(2)–N(41)	1.965(11)
Cu(1)–N(12)	2.015(11)	Cu(2)–N(32)	2.012(11)
Cu(1)–N(21)	2.027(10)	Cu(2)–N(42)	2.051(11)
Cu(1)–O(6)	2.239(9)	Cu(2)–O(20)	2.264(9)
N(11)–Cu(1)–N(22)	173.6(5)	N(31)–Cu(2)–N(41)	174.4(5)
N(11)–Cu(1)–N(12)	81.6(5)	N(31)–Cu(2)–N(32)	82.2(4)
N(22)–Cu(1)–N(12)	104.1(5)	N(41)–Cu(2)–N(32)	100.3(4)
N(11)–Cu(1)–N(21)	98.2(5)	N(31)–Cu(2)–N(42)	100.5(5)
N(22)–Cu(1)–N(21)	80.5(4)	N(41)–Cu(2)–N(42)	81.4(5)
N(12)–Cu(1)–N(21)	129.5(5)	N(32)–Cu(2)–N(42)	134.1(5)
N(11)–Cu(1)–O(6)	83.0(4)	N(31)–Cu(2)–O(20)	85.8(4)
N(22)–Cu(1)–O(6)	92.3(4)	N(41)–Cu(2)–O(20)	88.6(4)
N(12)–Cu(1)–O(6)	107.5(4)	N(32)–Cu(2)–O(20)	113.4(4)
N(21)–Cu(1)–O(6)	122.6(4)	N(42)–Cu(2)–O(20)	112.5(4)

positions are occupied by a nitrogen atom (Cu–N apical bonds and corresponding N–Cu–N angles: 1.978(11), 1.979(10) Å and 173.6(5)° for Cu(1); 1.960(11), 1.965(11) Å and 174.4(5)° for Cu(2), respectively). The equatorial plane is defined by an equilateral triangle consisting of two remaining nitrogen donors and an oxo group from the $\beta\text{-}[\text{Mo}_8\text{O}_{26}]^{4-}$ anion. The two Cu ions are approximately located on their equatorial planes (the deviations from the trigonal planes are 0.066 and 0.009 Å, respectively).

Similar to $[\{\text{Ni}(o\text{-phen})_2\}_2(\text{Mo}_8\text{O}_{26})]^{4-}$ and $[\{\text{Cu}(o\text{-phen})_2\}_2(\text{Mo}_8\text{O}_{26})]^{11-}$ compound **1** does not form an extended 1-D chain, 2-D layer, or 3-D structure. However, the linking manner between heterometallic group and octamolybdate unit in **1** is notably distinct from those observed for the above-mentioned complexes. In these two compounds and in those aforementioned organic–inorganic hybrid solids containing different $[\text{Mo}_8\text{O}_{26}]^{4-}$ isomers, the secondary transition metal complex subunits are attached to the octamolybdate surface by the

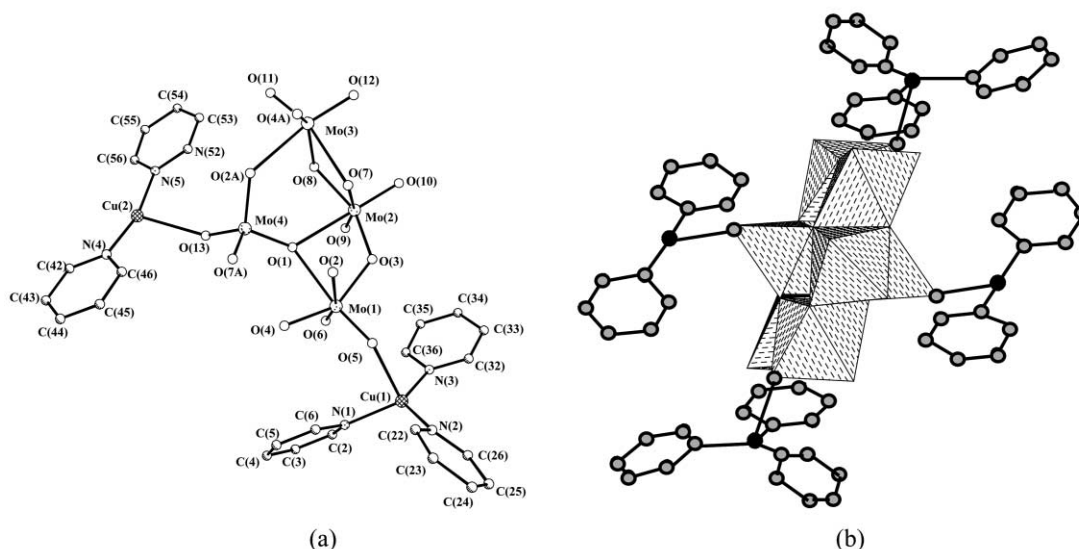


Fig. 2 (a) Asymmetrical unit and coordination environments of Cu atoms in **2**, with the atom-labeling scheme. (b) Polyhedral representation of the molecular structure of **2**.

Table 3 Selected bond lengths (Å) and angles (°) for $[\{\text{Cu}(\text{py})_3\}_2\{\text{Cu}(\text{py})_2\}_2(\alpha\text{-Mo}_8\text{O}_{26})]$ (**2**)

Cu(1)–N(3)	1.981(5)	Cu(2)–N(4)	1.902(4)
Cu(1)–N(2)	2.010(4)	Cu(2)–N(5)	1.916(4)
Cu(1)–N(1)	2.028(4)	Cu(2)–O(13)	2.398(3)
Cu(1)–O(5)	2.324(3)		
N(3)–Cu(1)–N(2)	125.22(19)	N(1)–Cu(1)–O(5)	91.28(15)
N(3)–Cu(1)–N(1)	120.11(19)	N(4)–Cu(2)–N(5)	165.79(19)
N(2)–Cu(1)–N(1)	111.98(18)	N(4)–Cu(2)–O(13)	97.86(15)
N(3)–Cu(1)–O(5)	97.49(17)	N(5)–Cu(2)–O(13)	94.52(15)
N(2)–Cu(1)–O(5)	97.13(16)		

terminal oxygen atoms of the same cluster anion. However, the $[\text{Cu}(2,2'\text{-bipy})]^{2+}$ complex cations in **1** are linked to the $\beta\text{-Mo}_8\text{O}_{26}$ anion *via* bridging oxo groups. This kind of linking manner represents an unusual example in the coordination chemistry of octamolybdates with transition metal complexes and even in that of the whole molybdenum-oxo clusters. It should be noted that compound **1** was prepared under similar conditions to that of $[\{\text{Ni}(2,2'\text{-bipy})\}_2(\beta\text{-Mo}_8\text{O}_{26})]$,¹² however, their structures differ significantly: **1** remains a discrete structure, while the $[\beta\text{-Mo}_8\text{O}_{26}]^{4-}$ anions in the latter complex are linked into a one-dimensional ribbon. This may originate from the nature of the employed heterometallic atoms. Ni(II) tends to adopt octahedral geometry whereas Cu(II) favors a four- or five-membered coordination geometry.

The crystal of **2** consists of centrosymmetric heterometallic dodecanuclear clusters $[\{\text{Cu}(\text{py})_3\}_2\{\text{Cu}(\text{py})_2\}_2(\alpha\text{-Mo}_8\text{O}_{26})]$ (**2**) (Fig. 2(a), Table 3), which are held together in an extended network *via* π - π stacking contacts. The common octamolybdate $[\alpha\text{-Mo}_8\text{O}_{26}]^{4-}$ anion in **2** is constructed from six MoO_6 octahedra and two MoO_4 tetrahedra. Six edge-sharing MoO_6 octahedra are co-planar to form a six-membered ring with either side being capped by a MoO_4 tetrahedron *via* corner sharing. Compound **2** has three kinds of Mo–O bonds: 1.692(3)–1.721(3) Å for Mo–O(t), 1.888(3)–1.928(3) Å for Mo–O(μ) and 1.772(3)–2.512(3) Å for Mo–O(μ_3).

Each $[\alpha\text{-Mo}_8\text{O}_{26}]^{4-}$ anion forms weak covalent interactions to two $[\text{Cu}(\text{py})_3]^+$ and two $[\text{Cu}(\text{py})_2]^+$ units through terminal oxo groups of the octamolybdate cluster. As shown in Fig. 2(a), the Cu(1) ion is linked to a terminal oxygen atom of an octahedral Mo site in the Mo_6O_6 ring [Cu–O: 2.324(3) Å] and three nitrogen atoms from three pyridine ligands [Cu–N: 1.981(5)–2.028(4) Å], and obviously leans toward the N_3 trigonal plane to form an elongated tetrahedron in the form of OCuN_3 . While for the $[\text{Cu}(\text{py})_2]^+$ unit, Cu(1) is linked to two pyridine ligands,

besides a terminal oxygen atom of a MoO_4 tetrahedron of the same octamolybdate anion, forming a “T”-shaped coordination geometry.

The crystal structure of **2** involves lattice engineering between cluster molecules. A remarkable feature of the structure is that two py groups of a $[\text{Cu}(\text{py})_2]^+$ unit are approximately co-planar (the mean and maximum deviations from the least-square plane defined by ten C and two N atoms of the two pyridine ligands are 0.085 and 0.166 Å, respectively) and the N–Cu–N angle deviates slightly from linearity. It is also notable that the adjacent $[\text{Cu}(\text{py})_2]^+$ units in **2** are generally parallel and separated by 3.015–3.324 Å, indicating π - π stacking interactions. The overall packing in **2** is given in Fig. 3, which shows how the

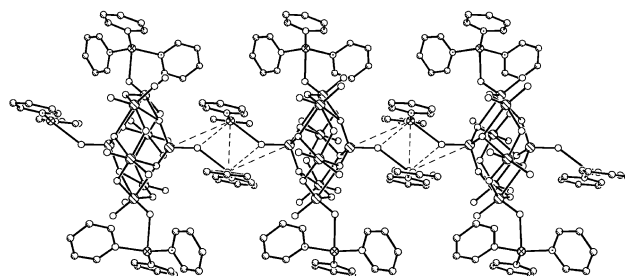


Fig. 3 Ball and stick representation of **2** viewed down the [001] direction, showing how the neighboring cluster molecules are connected into an infinite chain *via* π - π stacking interactions.

dodecanuclear heterometallic clusters of **2** are further extended into interesting one-dimensional supramolecular arrays *via* π - π stacking interactions of py ligands. Another important structural feature is that neighboring coordinated $[\text{Cu}(\text{py})_2]^+$ cations are within van der Waals contact of each other [Cu(2)–Cu(2)' = 3.149 Å].

Although a large number of Keggin structures with a formula described as $[(\text{XO}_4)\text{M}_{12}\text{O}_{36}]^{n-}$ (X = P, Si, Ge, As, V, etc.) have been synthesized and extensively used as important catalytic, medical and molecular materials, the first synthesis and structural characterization of the Keggin anion $[(\text{SO}_4)\text{Mo}_{12}\text{O}_{36}]^{2-}$ as the yellow NBU_4^+ salt was not reported until 1996.¹³ Its poor solubility has restricted a fuller characterization of reduced forms; the first one-electron-reduced $[(\text{SO}_4)\text{Mo}_{12}\text{O}_{36}]^{3-}$ species was synthesized and characterized by Wedd *et al.* in 2001.¹⁴ During the course of our attempt to synthesis new inorganic–organic hybrid oxide materials, a new compound $[\text{Cu}(\text{py})_2]_4[\text{Mo}^{\text{V}}_2\text{Mo}_{10}\text{O}_{36}(\text{SO}_4)]$ (**3**) with a two-electron-reduced

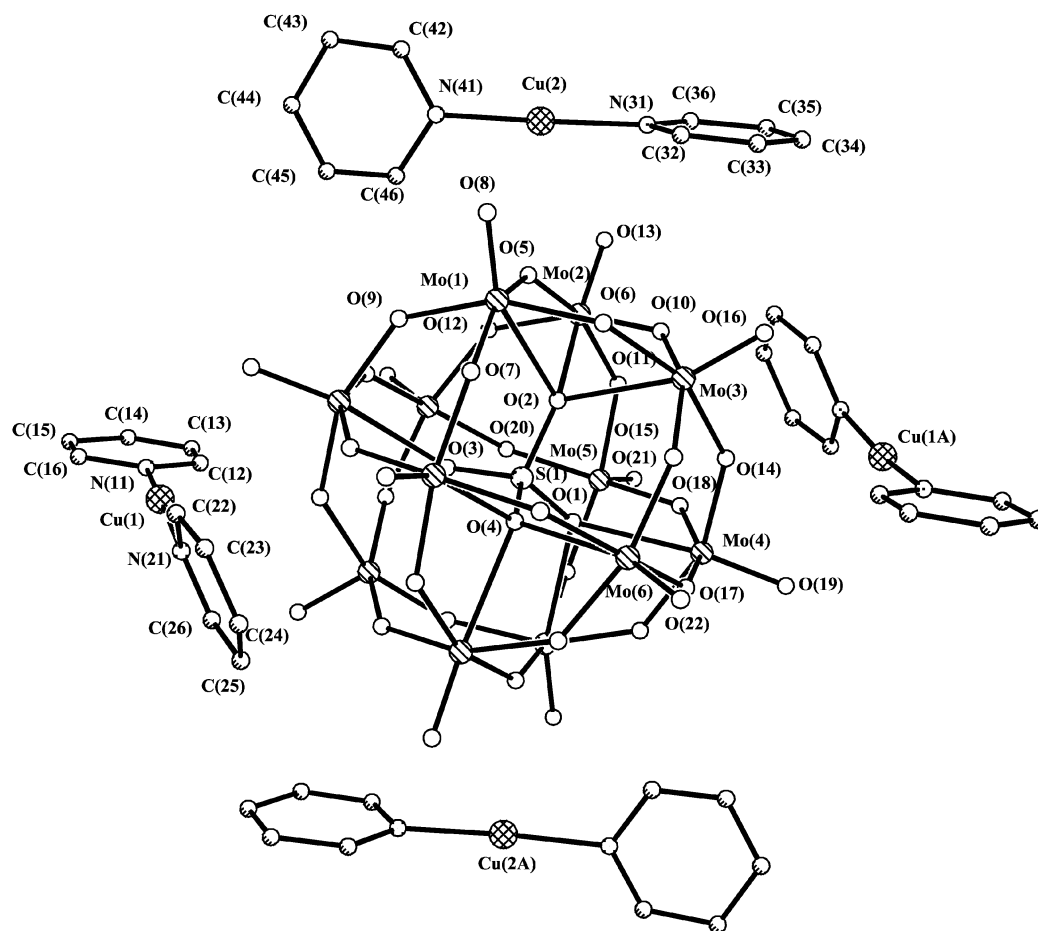


Fig. 4 Molecular drawing of **3**. The central S(1) atom is located at an inversion center surrounded by eight oxygen atoms with a partial occupancy of 0.5. (Four of the eight O atoms bonded to S(1) are omitted for clarity). Selected bond lengths: Cu(1)–N(11), 1.894(7), Cu(1)–N(21), 1.908(7), Cu(2)–N(31), 1.922(6), Cu(2)–N(41), 1.925(6). Symmetry operator: A $-x + 1, -y + 1, -z + 1$.

Table 4 Selected bond lengths (Å) and angles (°) for $[\text{Cu}(\text{py})_2]_2\text{-}[\text{Mo}_{12}\text{O}_{36}(\text{SO}_4)]$ (**3**)

Cu(1)–N(11)	1.894(7)	S(1)–O(1)#1	1.520(8)
Cu(1)–N(21)	1.908(7)	S(1)–O(1)	1.520(8)
Cu(2)–N(31)	1.922(6)	S(1)–O(4)	1.557(8)
Cu(2)–N(41)	1.925(6)	S(1)–O(4)#1	1.557(8)
S(1)–O(3)#1	1.507(8)	S(1)–O(2)#1	1.553(8)
S(1)–O(3)	1.507(8)	S(1)–O(2)	1.553(8)
N(11)–Cu(1)–N(21)	169.4(3)	O(1)–S(1)–O(4)#1	108.1(4)
N(31)–Cu(2)–N(41)	174.8(3)	O(3)–S(1)–O(2)#1	109.9(4)
O(3)#1–S(1)–O(1)#1	112.3(4)	O(1)–S(1)–O(2)#1	109.7(4)
O(3)–S(1)–O(1)	112.3(4)	O(4)#1–S(1)–O(2)#1	107.1(4)
O(3)#1–S(1)–O(4)	109.6(4)	O(3)#1–S(1)–O(2)	109.9(4)
O(1)#1–S(1)–O(4)	108.1(4)	O(1)#1–S(1)–O(2)	109.7(4)
O(3)–S(1)–O(4)#1	109.6(4)	O(4)–S(1)–O(2)	107.1(4)

Symmetry operator: #1 $-x + 1, -y + 1, -z + 1$.

Keggin anion was unexpectedly obtained from the hydrothermal reaction of a mixture of $\text{Na}_2\text{MoO}_4 \cdot 2\text{H}_2\text{O}$, $\text{CuSO}_4 \cdot 5\text{H}_2\text{O}$, nicotinic acid ($\text{py}-3\text{-CO}_2\text{H}$) and water in a molar ratio of 1.5 : 0.6 : 2.0 : 450. As shown in Fig. 4, the anion in **3** displays the classic Keggin structure consisting of one SO_4 tetrahedron and twelve MoO_6 octahedra (see Table 4 for selected bond lengths and angles). The Keggin anion in **3** may also be viewed as a shell of $\{\text{Mo}_{12}\text{O}_{36}\}$ encapsulating a central $\{\text{SO}_4\}$ moiety. The central S atom lies on an inversion center, and is surrounded by eight O oxygens with a partial occupancy of 0.5. Four $[\text{Cu}(\text{py})_2]^+$ cations with non-trivial two-fold coordination environments were found per $\text{SMo}_{12}\text{O}_{40}$ cluster, consistent with the presence of the two-electron-reduced anion $[\text{Mo}^{\text{V}}_2\text{Mo}^{\text{VI}}_{10}\text{O}_{36}(\text{SO}_4)]^{4-}$ in the crystals.

Commonly, Cu(i) exhibits a four-coordinate “tetrahedral” geometry, and there are a few reports on the trigonal-coordination Cu(i) complexes observed previously with cyanide ligands,^{15–17} or other mixed systems where the L–Cu–L angles are all nearly 120° .¹⁸ In addition to the $[\text{OCuN}_3]^+$ tetrahedra, a less-common example of the T-shaped $[\text{OCuN}_2]^+$ geometry was also observed in **2**. This may result from the stereochemical demand of lattice arrangements. It is easy to see from Fig. 3 that the steric hindrance between two neighboring cluster molecules increases notably, and the corresponding π – π stacking interactions between pyridine rings may be broken, when the Cu(i) ions are linked to the tetrahedral Mo atoms in a trigonal geometry. A viewpoint from a reputable standard text states that Cu(i) ions have a pronounced tendency to exhibit linear two-fold coordination.¹⁹ However, the results of extensive structural studies on Cu(i) complexes show that two-coordination is rather rare, being limited to complexes with σ -bonding and non-polarizable, or polarizable bulk ligands.^{20,21} Previous studies suggest that only alkyl substitution in both the 2- and 6-position of pyridine can further decrease the coordination number of Cu(i) to two,²² therefore to date, no structural data have been found for a two-coordinate copper(i) complex with pyridine. However, the present structure of $[\text{Cu}(\text{py})_2]_4\text{-}[\text{Mo}^{\text{V}}_2\text{Mo}^{\text{VI}}_{10}\text{O}_{36}(\text{SO}_4)]$ (**3**) shows that the Cu(i) ion can also form linear two-fold coordination complexes with polarizable non-bulky ligands under suitable conditions.

In conclusion, we have prepared and structurally characterized three new copper complexes: $[\{\text{Cu}(2,2'\text{-bipy})_2\}_2(\beta\text{-Mo}_8\text{O}_{26})]$ (**1**), $[\{\text{Cu}(\text{py})_3\}_2\{\text{Cu}(\text{py})_2\}_2(\alpha\text{-Mo}_8\text{O}_{26})]$ (**2**) and $[\text{Cu}(\text{py})_2]_4\text{-}[\text{Mo}_{12}\text{O}_{36}(\text{SO}_4)]$ (**3**). Although compound **1** does not form an extended structure, two interesting structural features are apparent: (1) the unique linking mode, *i.e.*, the $[\beta\text{-Mo}_8\text{O}_{26}]$

cluster anion bonding to the $[\text{Cu}(2,2'\text{-bipy})]^{2+}$ complex cations *via* bridging oxo groups, this represents a rare example in the coordination chemistry of octamolybdates and even in that of the whole coordination chemistry of molybdenum-oxo clusters; (2) the coordination geometry (trigonal bipyramidal) of the Cu(II) ions is also considerably rare. The structure of **2** is constructed from a $[\alpha\text{-Mo}_8\text{O}_{26}]^{4-}$ subunit bonded covalently to two $[\text{Cu}(\text{py})_3]^+$ and two $[\text{Cu}(\text{py})_2]^+$ coordination cations *via* terminal oxo groups. Compounds **2** and **3** are also interesting due to the very unusual Cu-coordination geometries: distorted tetrahedral, T-shaped trigonal, and linear Cu(I); in **2**, two distinct Cu(I)-coordination geometries are observed in the same structure!

Acknowledgements

The authors thank the Chinese Academy of Sciences, the National Science Foundation of China (20073048), and the Natural Science Foundation of Fujian for financial support.

References

- (a) M. T. Pope and A. Müller, *Angew. Chem., Int. Ed. Engl.*, 1991, **30**, 34–48; (b) For a recent overview on polyoxometalate chemistry refer to: *Chem. Rev.*, 1998, **98**, 1–387.
- P. J. Hagrman, D. Hagrman and J. Zubieta, *Angew. Chem., Int. Ed. Engl.*, 1999, **38**, 2638.
- Y. Zhang, P. J. Zapf, L. M. Meyer, R. C. Haushalter and J. Zubieta, *Inorg. Chem.*, 1997, **36**, 2159.
- J. Q. Xu, R. Z. Wang, G. Y. Yang, Y. H. Xing, D. M. Li, W. M. Bu, L. Ye, Y. G. Fan, G. D. Yang, Y. Xing, Y. H. Lin and H. Q. Jia, *Chem. Commun.*, 1999, 983.
- J. R. D. DeBord, R. C. Haushalter, L. M. Meter, D. Rose, P. J. Zapf and J. Zubieta, *Inorg. Chim. Acta*, 1997, **256**, 165.
- D. Hagrman, P. J. Zapf and J. Zubieta, *Chem. Commun.*, 1998, 1283.
- M. T. Pope, *Heteropoly and Isopoly Oxometalates*, Springer, New York, 1983.
- R. Xi, B. Wang, K. Isobe, T. Nishioka, K. Toriumi and Y. Ozawa, *Inorg. Chem.*, 1994, **33**, 833.
- D. Hagrman, C. Zubieta, D. J. Rose, J. Zubieta and R. C. Haushalter, *Angew. Chem., Int. Ed. Engl.*, 1997, **36**, 873.
- N. E. Brese and M. O'Keeffe, *Acta Crystallogr., Sect. B*, 1991, **47**, 192.
- P. J. Hagrman and J. Zubieta, *Inorg. Chem.*, 1999, **38**, 4480.
- P. J. Zapf, C. J. Warren, R. C. Haushalter and J. Zubieta, *Chem. Commun.*, 1997, 1543.
- T. Hori, S. Himeno and O. Tamada, *J. Chem. Soc., Dalton Trans.*, 1996, 2083.
- T. Vu, A. M. Bond, D. C. R. Hockless, B. Moubaraki, K. S. Murray, G. Lazarev and A. G. Wedd, *Inorg. Chem.*, 2001, **40**, 65.
- C. Kappenstein and R. P. Hugel, *Inorg. Chem.*, 1977, **16**, 250.
- S. Lopez and S. W. Keller, *Inorg. Chem.*, 1999, **38**, 1883.
- C. Kappenstein and R. P. Hugel, *Inorg. Chem.*, 1978, **17**, 1945.
- K. T. Potts, C. P. Horwitz, A. Fessak, M. Keshavarz-K, K. E. Nash and P. J. Toscano, *J. Am. Chem. Soc.*, 1993, **115**, 10444.
- F. A. Cotton and G. Wilkinson, *Advanced Inorganic Chemistry*, 4th edn., John Wiley and Sons, New York, 1980, p. 969.
- Y. Agnus, R. Louis and R. Weiss, *J. Chem. Soc., Chem. Commun.*, 1980, 867.
- M. J. Schillistra, P. J. M. W. L. Birker, G. C. Verschoor and J. Reedijk, *Inorg. Chem.*, 1982, **21**, 2637.
- L. M. Engelhardt, C. Pakawatchai and A. H. White, *J. Chem. Soc., Dalton Trans.*, 1985, 117.
- G. M. Sheldrick, SADABS, Siemens Analytical X-Ray Instrument Division, Madison, WI, 1995.